

## THE PRESENT AND THE FUTURE OF COSMOLOGY WITH GAMMA RAY BURSTS

G. GHIRLANDA & G. GHISELLINI

*Osservatorio Astronomico di Brera  
Via E. Bianchi 46  
I-23807 Merate (LC)  
E-mail: ghirla@merate.mi.astro.it*

Gamma Ray Bursts are among the most powerful astrophysical sources and they release up to  $10^{54}$  erg, if isotropic, in less than few hundred seconds. Their detection in the hard X/ $\gamma$  ray band (at energies  $\geq 10$  keV) and out to very high redshift ( $z \approx 6.3$ ) makes them a powerful new cosmological tool (a) to study the reionization epoch, (b) to unveil the properties of the IGM, (c) to study the present universe geometry and (d) to investigate the nature and cosmic evolution of the dark energy. While GRBs will surely help to understand the first two issues in the future, the present link between GRBs and cosmology has been made *concrete* by the recent discovery of a tight correlation between their rest frame prompt and afterglow emission properties which allowed their use as *standard candles*.

### 1. Introduction

Since their discovery in the latest sixties, the observational picture of GRBs have been enriched with new pieces of evidence relative to their emission properties, distance scale and intrinsic properties. Also the theoretical models which pretend to interpret these results were refined (e.g. see <sup>19</sup> for a recent review).

The nature of GRB progenitors, the huge amount of energy emitted during their prompt and afterglow phase, their relativistic nature and their cosmological distance scale makes them one of the most *interdisciplinary* field of research in modern astrophysics. Their study, in fact, requires concepts and methods drawn from the field of stellar evolution, of the physics of compact objects and of relativistic plasmas, of radiative process and they also represent a laboratory to test general relativity and a new tool for cosmology.

The last point gathered the interest of the scientific community since the settlement of the cosmological distance scale of the class of long duration

(i.e.  $\geq 2$  sec) GRBs in 1997<sup>3</sup>. In fact, the large luminosity of GRBs and their redshift extension ( $z \sim 6.3$  up to Sept. 2005<sup>11</sup>) makes them the brightest distant objects we know of, rising our hopes to test different cosmological models and to study the nature of dark energy<sup>(8)</sup>, i.e. some of the hottest topics of modern cosmology.

## 2. From the isotropic energy to the collimation corrected energy

Apparently GRBs are all but standard candles: for  $\sim 30$  bursts with measured redshift  $z$  and fluence  $F$  (integrated over the rest frame 1keV–10MeV energy range) the *isotropic equivalent energy* results,

$$E_{\text{iso}} = \frac{4\pi d_L(z)^2}{(1+z)} F \quad (1)$$

with an average value  $\sim 10^{53}$  erg and a wide spread over  $\sim 3$  orders of magnitudes.

However, we know that GRBs are collimated sources with a typical opening angle  $\theta_{\text{jet}}$  of few degrees<sup>4</sup>. The estimate<sup>18</sup> of the jet opening angle is allowed by the measure of the achromatic jet break time  $t_{\text{break}}$ , i.e. the time (typically between 0.5 and 6 days<sup>13</sup>) when the afterglow light curve steepens. The link between  $t_{\text{break}}$  and  $\theta_{\text{jet}}$  is shown in Fig.1. Due to the relativistic beaming of the photons emitted by the fireball, the observer perceives the photons within a cone with aperture  $\theta_{\Gamma} \propto 1/\Gamma$  where  $\Gamma$  is the bulk Lorentz factor of the material responsible for the emission. During the afterglow phase the fireball is decelerated by the ISM and its bulk Lorentz factor decreases, i.e. the beaming angle  $\theta_{\Gamma}$  increases, with time. A critical time is reached when the beaming angle equals the jet opening angle, i.e.  $\theta_{\Gamma} \sim 1/\Gamma \sim \theta_{\text{jet}}$ , when the entire jet surface is visible any further increase of the beaming angle (due to a decrease of the bulk Lorentz factor) does not increase the visible surface any longer. This time corresponds to a change (steepening) of the afterglow light curve as schematically represented in Fig.1.

The measure of  $\theta_{\text{jet}}$  allows to correct  $E_{\text{iso}}$  and derive the *collimation corrected energy*,

$$E_{\gamma} = E_{\text{iso}}(1 - \cos \theta_{\text{jet}}) \quad (2)$$

which is however spread over 2 orders of magnitudes and does not make GRBs standard candles.

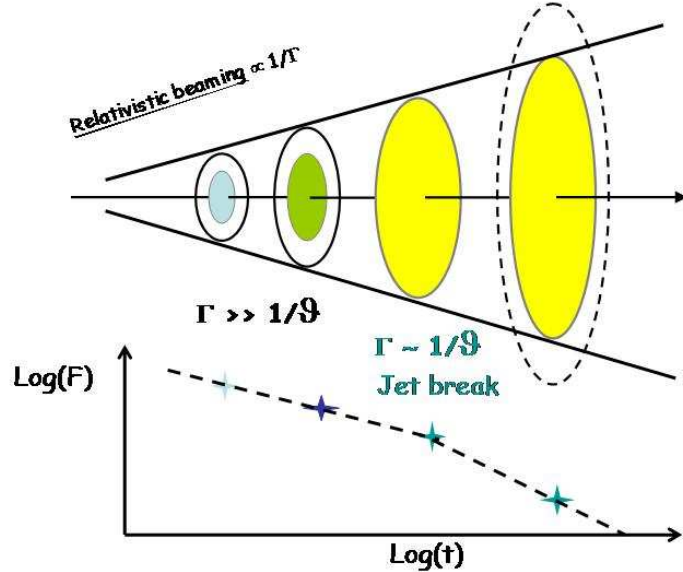


Figure 1. Cartoon of the relation between the jet break time appearing in the afterglow light curve (bottom panel) and the jet opening angle. The shaded surfaces represent the area corresponding to the beaming angle of the photons from which the observer perceives the emitted radiation. When  $1/\Gamma \sim \theta_{\text{jet}}$  a change in the decay slope of the afterglow light curve appears.

The GRBs whose prompt emission spectrum is known over a wide energy range so that their peak spectral energy  $E_{\text{peak}}$  (i.e. the peak of the  $EF_E$  spectrum) is properly constrained, present a correlation<sup>1</sup> between  $E_{\text{peak}}$  and  $E_{\text{iso}}$ . With the present sample of 29 GRBs<sup>13</sup> (updated with GRB 051022 -<sup>14</sup>) with accurately measured  $z$ ,  $E_{\text{peak}}$  and fluence we find (assuming a standard cosmology with  $\Omega_M = 0.3$ ,  $\Omega_\Lambda = h = 0.7$ ):

$$\left( \frac{E'_p}{100 \text{ keV}} \right) = (2.34 \pm 0.01) \left( \frac{E_{\text{iso}}}{2.76 \times 10^{52} \text{ erg}} \right)^{0.54 \pm 0.02} \quad (3)$$

with a reduced  $\chi^2 = 4.97$  (27 dof) (Fig.2). The scatter defined by the 29 data points in the  $E_{\text{peak}}-E_{\text{iso}}$  plane around the correlation defined in Eq.(3) is well represented by a gaussian distribution with  $\sigma = 0.25$  dex.

If we instead correct the isotropic energy for the collimation angle  $\theta_{\text{jet}}$  as defined in Eq.(2), a *tighter correlation* between  $E_{\text{peak}}$  and  $E_{\text{iso}}$  is found<sup>7</sup>.

The GRBs for which the jet break time has been measured from the

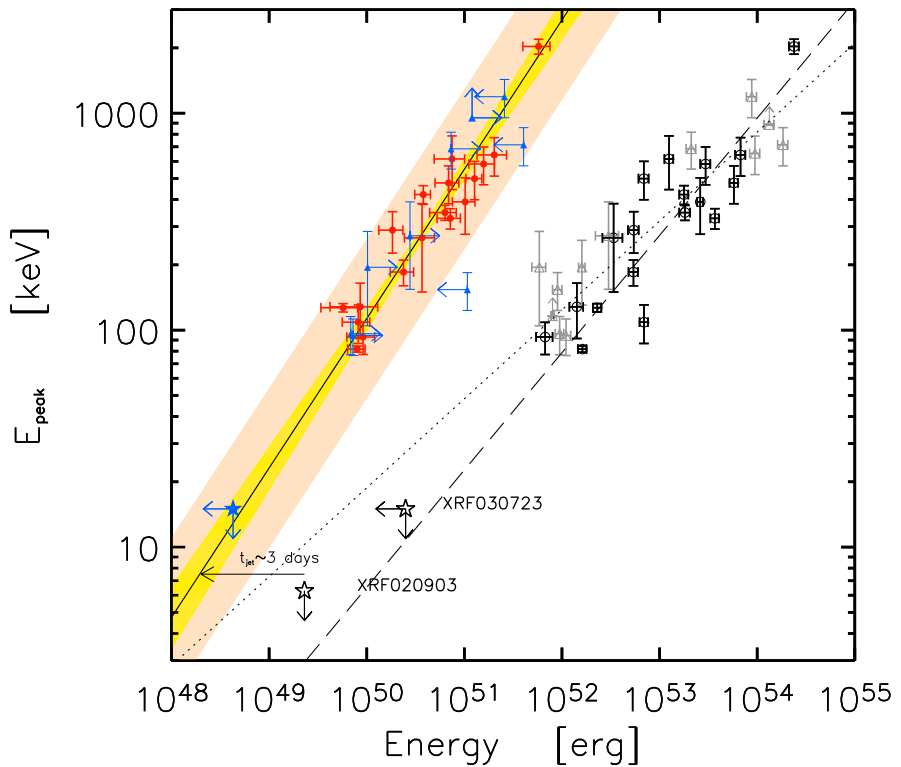


Figure 2. Rest frame peak energy  $E_{\text{peak}}$  versus isotropic (open symbols) and collimation corrected (filled symbols) energy. The black open circles are the 19 GRBs with measured  $z$ ,  $E_{\text{peak}}$  and  $t_{\text{jet}}$  for which the collimation corrected energy could be computed (red filled circles). Upper/lower limits on either one of the variables are shown by the blue filled triangles. The best fit powerlaw to the red filled circles - Eq.(4) - is represented by the solid line and its uncertainty by the thin yellow shaded region. The large (light orange) shaded region represents the  $3\sigma$  gaussian scatter of the data points around the correlation. Also shown is the  $E_{\text{peak}} - E_{\text{iso}}$  correlation obtained by fitting the open black data points and the open grey triangles (which are not upper/lower limits) either accounting for the errors on both the coordinates (long dashed line - slope = 0.54 and  $\chi^2_{\text{r}} = 4.9$  for 27 dof) and by a linear regression (dotted line - slope = 0.4).

afterglow light curve allows to derive the jet opening angles. To the original sample of 15 bursts of 7 other 4 bursts have been added: GRB 021004, GRB 041006, GRB 050525 and GRB 051022. The correlation defined with

this updated sample of 19 GRBs is:

$$\left( \frac{E'_p}{100 \text{ keV}} \right) = (2.82 \pm 0.02) \left( \frac{E_\gamma}{3.72 \times 10^{50} \text{ erg}} \right)^{0.69 \pm 0.04} \quad (4)$$

which gives a better fit (with respect to Eq.(3)), i.e. a reduced  $\chi^2 = 1.32$  (17 dof) (Fig.2). Also the scatter defined by the 19 data points in the  $E_{\text{peak}}-E_{\text{iso}}$  plane around the correlation defined in Eq.(4) is well represented by a gaussian distribution with  $\sigma = 0.1$  dex.

### 3. Constraints on the cosmological parameters

The tight  $E_{\text{peak}}-E_\gamma$  correlation makes GRBs standard candles in the sense that, similarly to the stretching-luminosity correlation of SNIa, allows to derive the GRB true energy. In fact, the correlation represents the concrete possibility to use GRBs to test the cosmological parameters and to study the nature of dark energy. In fig.3 we show the constraints on the  $\Omega_M, \Omega_\Lambda$  parameters obtained with the sample of 19 GRBs.

Although the contours obtained with 19 GRBs are shallow due to the low number of bursts (only 19) compared to SNIa, we can see that GRB constraints are complementary to those defined by SNIa and CMB in the  $\Omega_M-\Omega_\Lambda$  parameter space. GRBs are detected out to very high redshifts (the present highest detected  $z \sim 6.3$  which unfortunately has an unconstrained peak energy) and therefore they can give better constraints in combination with the other cosmological probes.

### 4. The future of cosmology with GRBs

Two urgent open issues related to the use of GRBs for cosmology are (i) the circularity problem<sup>10</sup> and (ii) the small number of the present sample of GRBs with measured  $z$ ,  $E_{\text{peak}}$  and  $t_{\text{break}}$ .

(i) The luminosity distance which allows to compute  $E_{\text{iso}}$  in Eq.(1) (and  $E_\gamma$  from Eq.(2)) is derived by assuming a cosmological model (defined by the  $\Omega = (\Omega_M, \Omega_\Lambda)$  parameters). Therefore, the slope and normalization of the correlation, i.e.  $E_{\text{peak}} = KE_\gamma^g$ , depend on the particular cosmological model adopted, i.e.  $K(\Omega)$  and  $g(\Omega)$ , and we cannot use the correlation found in a particular cosmology (e.g.  $\Omega_M = 0.3, \Omega_\Lambda = 0.7$ ) to derive the constraints on the cosmological parameters. A method<sup>7</sup> that circumvents this “circularity” problem is based on fitting the correlation in every cosmology and finding the cosmologies (i.e. the  $\Omega$  values) which minimize the

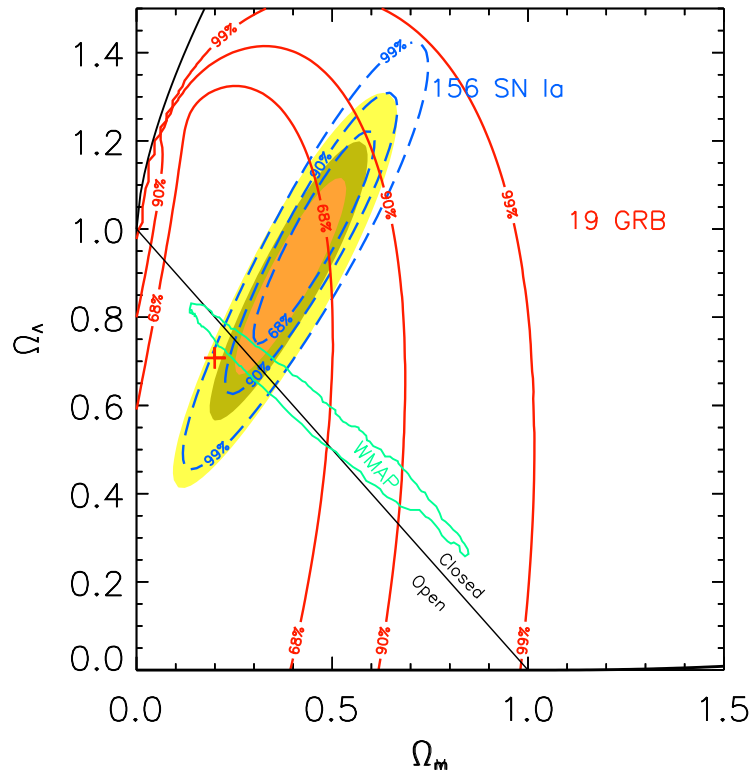


Figure 3. Constraints (1,2 and  $3\sigma$ ) on the cosmological parameters  $\Omega_M, \Omega_\Lambda$  obtained with the 19 GRBs with  $z$ ,  $E_{\text{peak}}$  and  $t_{\text{break}}$  measured (solid contours). The contours obtained with the 156 SNIa of the Gold sample are also shown (long-dashed contours) and the combined GRB+SNIa contours (shaded regions) are represented. Also shown are the 90% constraints obtained with the WMAP data.

$\chi^2$  of the fit. A more refined method based on Bayes theorem has been proposed and applied<sup>5</sup>. However these methods have the inconvenience that the resulting constraints are less stringent than in the case that the slope  $g$  and normalization  $K$  of the correlation could be fixed (i.e. cosmology independent). The latter situation can be realized either if the correlation is calibrated with a sample of low redshift GRBs, i.e. at redshifts  $< 0.1$ , or if its theoretical interpretation is found. In both cases in fact, the slope and normalization would become independent of  $\Omega$ . We stress that the require-

ment of having low redshift GRBs is not so stringent: we estimate <sup>9</sup> that a sample of 12 GRBs with redshift  $z \in (0.9, 1.1)$  can be used to calibrate the correlation with a precision better than 1% (i.e. the same accuracy achieved with 12 bursts with  $z \in (0.45, 0.75)$ ). A valid alternative is to find a solid theoretical interpretation of the correlation which would fix the values of  $K$  and  $g$  independently from the cosmological parameters.

(ii) A simulation of a sample of 150 GRBs shows <sup>9</sup> that the  $1\sigma$  constraints obtained with GRBs alone might improve of roughly a factor 10 with respect to the present constraints obtained with only 19 bursts (solid contours in Fig.3). However, the increase of the sample of GRBs used in cosmology represents an issue<sup>12</sup> because, for every GRB which is added to the sample of 19 we need to measure: (i) the redshift  $z$ ; (ii) the jet break time  $t_{\text{break}}$  from the X-ray/Optical light curve (this measure requires the monitoring of the GRB light curve up to  $\sim 10$  - depending on the redshift of the source  $z$ ) (iii) the peak energy of the prompt emission  $E_{\text{peak}}$

In particular the measure of  $E_{\text{peak}}$  requires to have a spectrum of the prompt emission of the burst over a wide energy range. In fact, we know that GRB spectra are characterized by a featureless continuum which is often represented <sup>2</sup> by a double smoothly-joined powerlaw model. Typically the  $EF_E$  spectrum shows a peak at  $\approx 300$  keV <sup>15</sup> and it has been shown to be extended to very low values (i.e.  $\approx 20$  keV) by the class of X-Ray Flashes <sup>17</sup>. Therefore a detector which can cover the 10 keV–1MeV energy range is required <sup>12</sup> to constrain  $E_{\text{peak}}$ .

Among the presently flying instruments catching GRBs, Swift has the highest detection rate ( $\sim 1$  GRB every 3 days roughly) as it was specifically designed to detect and monitor the burst on-the-fly to pinpoint its position with a high accuracy <sup>6</sup> (to better than  $\sim 5''$  in the X-ray band). However, the limited energy range (15–150 keV) of the high energy instrument on board Swift does not allow to constrain the peak energy of most GRBs it detects. However, the IPN satellites and Hete-II <sup>12</sup> have better chances to measure the  $E_{\text{peak}}$  parameter and, as it appeared from the recent case of GRB 051022, their joint work with Swift might be the key to collect some more GRBs to be added to the presently small sample of GRBs used as standard candles.

### Acknowledgments

A. Celotti, C. Firmani, D. Lazzati and F. Tavecchio are thanked for continuous stimulating discussions. The Italian MIUR is thanked for funding

(cofin grant 2003020775\_002)

### References

1. L. Amati et al. *A&A* **390**, 81 (2002)
2. D. Band et al. *ApJ* **413**, 281 (1993)
3. S. G. Djorgovski *IAU Circ.*, **6660** (1997)
4. D. A. Frail *ApJ* **534**, 559 (2000)
5. C. Firmani et al. *MNRAS* **360**, L1 (2005)
6. N. Gherels et al. *ApJ* **611**, 1005 (2004)
7. G. Ghirlanda, G. Ghisellini & D. Lazzati, *ApJ* **616** 331 (2004)
8. G. Ghirlanda et al. *ApJ*, **613**, L13 (2004)
9. G. Ghirlanda et al. *MNRAS* submitted
10. G. Ghisellini et al. *Il Nuovo Cimento* in press (2005)
11. N. Kawai et al. *GCN Circ.* **3937** (2005)
12. D. Lamb et al. *White paper submitted to the Dark Energy Task Force* astro-ph/0507362 (2005)
13. L. Nava et al. *ApJ*, submitted (2005)
14. Olive F. et al. *GCN Circ.* **4131** (2005)
15. R. D. Preece et al. *ApJS* **126**, 19 (2000)
16. A. G. Riess et al. *ApJ* **607**, 665 (2004)
17. T. Sakamoto et al. *ApJ* **629**, 311 (2005)
18. R. Sari *ApJ* **519**, L17 (1999)
19. B. Zhang & P. Meszaros, *IJMPA* **19**, 2385 (2004)